^1H, ^{13}C and ^{15}N Nuclear magnetic resonance analysis and chemical features of the two main radical oxidation products of 2′-deoxyguanosine: oxazolone and imidazolone nucleosides

Sébastien Raoul,[a] Maurice Berger,[a] Garry W. Buchko,[b] Prakash C. Joshi,[c] Bénédicte Morin,[a] Michael Weinfeld[b] and Jean Cadet*,†,[a]

[a] *CEA/Département de Recherche Fondamentale sur la Matière Condensée, SCIB/LAN, F-38054 Grenoble Cedex 9, France*
[b] *Department of Radiobiology, Cross Cancer Institute, 11560 University Ave., Edmonton, Alberta, T6G 1Z2, Canada*
[c] *Industrial Toxicology Research Centre, PO Box 80, Lucknow-226 001, India*

The two primary one-electron oxidation and ·OH-mediated decomposition products of 2′-deoxyguanosine 1 are 2,2-diamino-4-[(2-deoxy-β-D-*erythro*-pentofuranosyl)amino]-2,5-dihydrooxazol-5-one 3 (dZ) and its precursor, 2-amino-5-[(2-deoxy-β-D-*erythro*-pentofuranosyl)amino]-4*H*-imidazol-4-one 2 (dIz). Here, we describe in detail the spectroscopic and chemical properties of both oxidative DNA lesions. The structures for dZ 3 and dIz 2 were determined by fast-atom bombardment mass spectrometry, UV spectroscopy, IR spectroscopy, together with ^1H, ^{13}C, ^{15}N and ^{17}O 1D and 2D NMR spectroscopy. In neutral aqueous solution dIz 2 is hydrolysed to dZ 3 ($t_{\frac{1}{2}}$ = 147 min at 37 °C) with the incorporation of one molecule of water. Hot alkali treatment (65 °C; pH 13) of dIz 2 and dZ 3 quantitatively results in the release of guanidine ($t_{\frac{1}{2}}$ = 3.3 and 3.1 min, respectively). The latter property allowed us to develop a specific and sensitive method for the detection of the two modified nucleosides 2 and 3. Methoxyamine reacts quantitatively with 3′,5′-di-*O*-acetyl-dIz 2a 120-times faster than with 3′,5′-di-*O*-acetyl-dZ 3a to form four 3,5-di-*O*-acetyl-2-deoxy-D-*erythro*-pentose–methoxyamine isomers.

Introduction

Oxidation reactions of DNA, a critical cellular target, are known to be involved in mutagenesis, carcinogenesis and lethality.[1] Oxidative DNA damage includes base modifications, abasic sites, DNA strand breaks and DNA–protein adducts.[2] Most of them are induced by reactive oxygen species and radical processes generated under various conditions of oxidative stress.[3] A particularly reactive species which is always present in living cells, the ·OH radical, is to a considerable extent responsible for such damage. The reactions of ·OH with purine and pyrimidine nucleosides have been extensively studied by pulse radiolysis techniques during the past decade (for a comprehensive review, see Steenken[4]). Another source of oxidative DNA damage involves UV-A radiation or visible light associated with an endogenous photosensitizer. Such oxygen-dependent photosensitization processes occur through two competitive mechanisms.[5] Type I mechanism requires either initial electron transfer or hydrogen abstraction by the sensitizer in the excited triplet state from the substrate (DNA bases) to generate free radicals. Type II mechanism involves the formation of singlet oxygen by energy transfer from the photoexcited sensitizer to triplet ground-state molecular oxygen. Then, $^1O_2$ reacts with the appropriate substrate.[6] Among the four DNA bases, guanine is known to be the most easily oxidized[7,8] by both ·OH-mediated reaction and photosensitization, including Type I and singlet-oxygen reactions.[9,10] This is explained by the fact that guanine has the lowest ionization potential. In addition, it is assumed that positive holes created in DNA by ionizing radiation or other oxidizing agents ultimately end up at guanine.[11–13]

While the structure and redox properties of the primary radicals of 2′-deoxyguanosine **1** (dGuo) have recently been established,[14] only limited information is available on the main final oxidation products with the exception of 2′-deoxy-8-oxo-7,8-dihydroguanosine **4** (8-oxodGuo).[15–17] In addition to recently published preliminary accounts,[9,10] we wish to report further spectroscopic data and chemical properties on the two predominant radical oxidation products of the base moiety of dGuo **1** arising from either Type I photosensitization or ·OH radical oxidation under oxic conditions. The two products have been characterized as 2,2-diamino-4-[(2-deoxy-β-D-*erythro*-pentofuranosyl)amino]-2,5-dihydrooxazol-5-one **3** (dZ) and its precursor, 2-amino-5-[(2-deoxy-β-D-*erythro*-pentofuranosyl)-amino]-4*H*-imidazol-4-one **2** (dIz).

A likely mechanism for the formation of the two latter

† **E-mail**: cadet@drfmc.ceng.cea.fr

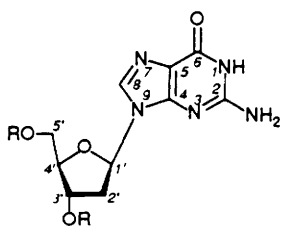

R=H dGuo 1
R=Ac 1a

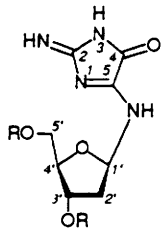

R=H dIz 2
R=Ac 2a

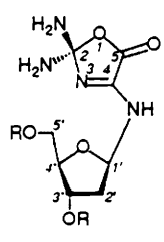

R=H dZ 3
R=Ac 3a

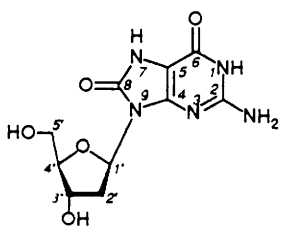

8-oxodGuo 4

oxidation products involves the initial addition of 'OH at C-4, followed by a dehydration reaction leading to the formation of the oxidizing neutral radical.[4] Subsequent addition of molecular oxygen occurs at the C-5 position of a tautomeric form of the neutral radical as inferred from the incorporation of heavy oxygen in compounds **2** and **3** when photosensitization experiments were performed in $^{18}O_2$-saturated solutions.[9] This is followed by the opening of the pyrimidine ring and subsequent rearrangements. Identical reactions are likely to take place following the deprotonation of the guanine radical cation after its initial formation from one-electron oxidation, *e.g.* by Type I photosensitization (Scheme 1). It should be noted that under these conditions the yield of formation of 8-oxodGuo **4** never exceeds 0.8% at the nucleoside level, and represents only a minor product of the radical oxidation of dGuo **1**.

Results and discussion

Chromatographic features and isolation of both imidazolone 2 and oxazolone 3 derivatives

Benzophenone-mediated photooxidation of dGuo **1**, which predominantly involves a Type I mechanism, generates dZ **3** and its precursor dIz **2** (*vide infra*) as the main decomposition products. HPLC isolation of dZ **3** was achieved on a silica gel NH_2 column as previously described.[18] It should be added that the imidazolone derivative dIz **2**, the precursor of **3**, coelutes with the starting dGuo **1** under these conditions. However, an alternative way to obtain a large amount of pure dZ **3** for spectroscopic analyses was to isolate dIz **2** prior to its hydrolytic transformation. This was achieved by preparative reversed-phase HPLC with water as the eluent. The fraction containing dIz **2** was then either quickly lyophilized to obtain a homogenous product or left in aqueous solution at room temperature for 48 h in order to convert quantitatively dIz **2** into dZ **3** (*vide infra*). However, the second approach requires separation of the photooxidation products of dGuo **1** immediately after UV-A photosensitization in order to minimize hydrolysis of dIz **2**.

Structure determination of dIz 2 and dZ 3

Mass spectrometry. The positive fast-atom bombardment mass spectrum (FAB-MS) of dZ **3** exhibits a pseudomolecular ion at *m/z* 247.2 ($[M + H]^+$) together with a fragment at *m/z* 131.1 ($[BH + H]^+$) which corresponds to the aglycone. The presence of the characteristic fragment of the sugar moiety at *m/z* 117.0 ($[S]^+$) indicates that the modification occurred within the base moiety. Exact mass measurement of the pseudomolecular ion (*m/z* 247.1152) reveals an elemental composition of $C_8H_{14}N_4O_5$ for the nucleoside. During the radical oxidation of the starting dGuo **1**, two carbons and one nitrogen are lost whereas one hydrogen and one oxygen atom are gained. The exact mass of dIz **2** was 229.0929, corresponding to a molecular formula of $C_8H_{12}N_4O_4$ for the nucleoside. It should be noted that there is a gain of one molecule of H_2O upon conversion of dIz **2** into dZ **3**. Additional support for the incorporation of one molecule of H_2O was inferred from the hydrolysis of dIz **2** using isotopically enriched water $H_2{}^{18}O$. The exact mass measurement of ^{18}O-labelled dZ **3** reveals a pseudomolecular ion at *m/z* 249.1097 (theoretical calculation 249.1085). The latter experiment also provides further confirmation for the mechanism of hydrolysis of dIz **2** into dZ **3**.

^{1}H NMR spectroscopy. The ^{1}H NMR data obtained in D_2O (Table 1) show that the sugar moiety of dZ **3** and dIz **2** remains intact. It should be added that no drastic differences in the ^{1}H NMR features of both compounds **2** and **3** are observable with the exception of a slight downfield shift for the signals of the sugar protons of dIz **2** with respect to those of dZ **3**. Analysis of the sugar coupling constants of compounds **2** and **3** allows the unambiguous assignment of their β anomeric furanose configuration (Fig. 1). The relatively large *trans* coupling constant $J_{1'-2'}$ associated with the low value of the two other *trans* coupling constants $J_{2''-3'}$ and $J_{3'-4'}$ suggest that the sugar preferentially adopts a C-2′ *endo* puckered conformation.[19,20] In such a conformation, 3′-H is involved in two *trans* diequatorial orientations with 4′-H and 2″-H. In addition, a slight destabilization of the *gauche-gauche* rotameric population of the 5′-OH group, with respect to the starting dGuo **1**, is inferred from the higher $J_{4'-5'}$ and $J_{4'-5''}$ sum ($\Sigma \approx 9.5$ Hz)[21] for both compounds **2** and **3** relative to dGuo **1** ($\Sigma \approx 8.4$ Hz).

Concerning the base moiety of both dZ **3** and dIz **2**, the lack of the 8-H resonance signal in the low-field region of the spectrum indicates that the purine ring of the nucleoside has been modified. The 0.43 ppm (0.35 ppm) upfield shift observed for 1′-H and 2′-H of dZ **3** (dIz **2**, respectively) with respect to dGuo **1** may be explained by the loss of aromaticity of the base moiety. Indeed, the aromatic ring current is known to induce a downfield shift on the two latter protons.[22]

Inspection of the ^{1}H NMR features of dZ **3** and dIz **2** obtained in $(CD_3)_2SO$ ([$^2H_6$]DMSO) (Table 2) confirms the β furanose configuration of the sugar moiety for both compounds. Interestingly, an exchangeable resonance signal with a large coupling constant [^3J(H,H) = 9.1 Hz for **3** and ^3J(H,H) = 7.3 Hz for **2**] resonates at $\delta = 8.18$ for **3** and $\delta = 9.32$ for **2**. The latter signals were assigned as that of 4-NH for dZ **3** and 5-NH for dIz **2**, respectively, on the basis of homonuclear decoupling experiments performed on the

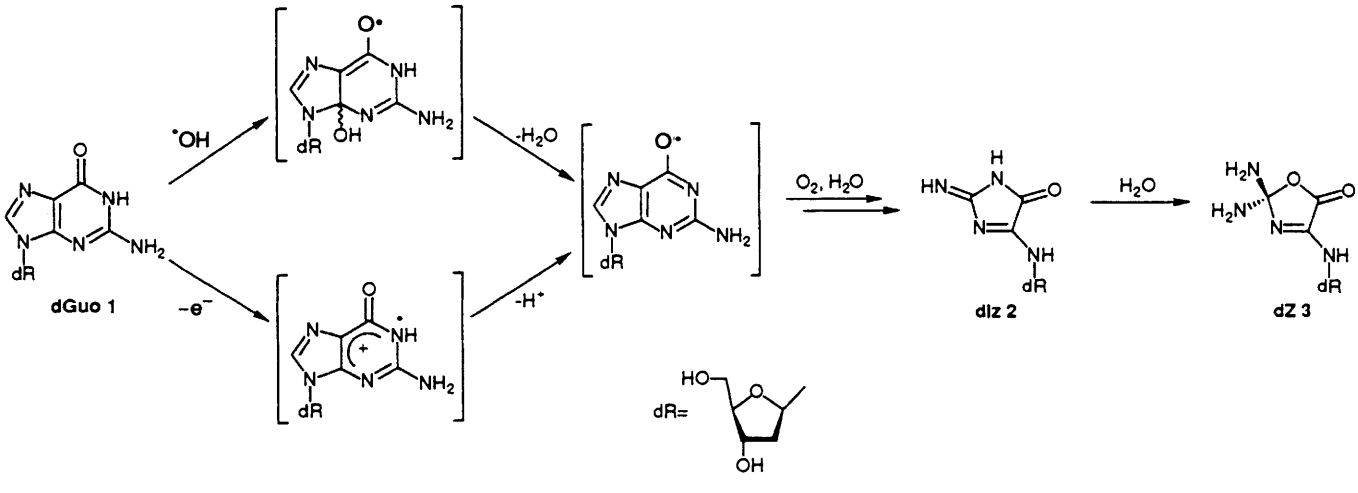

Scheme 1 Formation of dIz **2** and dZ **3** upon radical oxidation of dGuo **1** arising from either Type 1 photosensitization (one-electron oxidation) or γ-irradiation ('OH radical)

Table 1 400.13 MHz ^{1}H NMR chemical shifts (ppm) and coupling constants[a] (Hz) of dGuo **1**, dZ **3** and dIz **2** obtained in D_2O

δ(ppm)	1′-H	2′-H	2″-H	3′-H	4′-H	5′-H	5″-H	8-H
dGuo **1**	6.30	2.79	2.52	4.64	4.14	3.82	3.77	7.99
dZ **3**	5.87	2.36	2.38	4.51	4.06	3.77	3.72	
dIz **2**	5.95	2.45	2.47	4.55	4.13	3.79	3.74	

J_{i-j} (Hz)	$J_{1'-2'}$	$J_{1'-2''}$	$J_{1'-3'}$	$J_{2'-2''}$	$J_{2'-3'}$	$J_{2''-3'}$	$J_{3'-4'}$	$J_{4'-5'}$	$J_{4'-5''}$	$J_{5'-5''}$
dGuo **1**	7.4	6.3	n.d.[b]	−14.1	6.1	3.6	2.6	3.7	4.7	−12.6
dZ **3**	6.9	6.5	0.3	−14.0	6.2	3.2	2.9	4.2	5.4	−12.3
dIz **2**	6.6	6.3	0.4	−14.0	6.1	3.7	3.1	4.1	5.3	−12.3

[a] Estimated errors ±0.1 Hz. [b] Not determined.

Table 2 250.13 MHz ^{1}H NMR chemical shifts (ppm) of dGuo **1**, dZ **3** and dIz **2** obtained in [$^2H_6$]DMSO

(A) Sugar moiety

δ(ppm)	1′-H	2′-H	2″-H	3′-H	4′-H	5′-H_2[a]	5′-OH	3′-OH
dGuo **1**	6.23	2.61	2.30	4.45	3.92	3.65	5.10	5.41
dZ **3**	5.75	2.19	1.99	4.27	3.77	3.50	4.90	5.15
dIz **2**	5.82	2.32	2.12	4.32	3.83	3.52	4.92	5.22

(B) Base moiety

δ(ppm)	8-H	1-NH	NH_2	4-NH	5-NH	3-NH	2-NH
dGuo **1**	8.05	10.78	6.59				
dZ **3**			7.62[b]	8.18[c]			
dIz **2**					9.32[c]	8.94	9.06

[a] The broad signal of residual water masks, at least partly, these signals and makes the exact assignment of these two protons difficult. [b] For symmetry reasons, the four protons of the two NH_2 groups resonate at the same frequency. [c] These signals appear as a doublet.

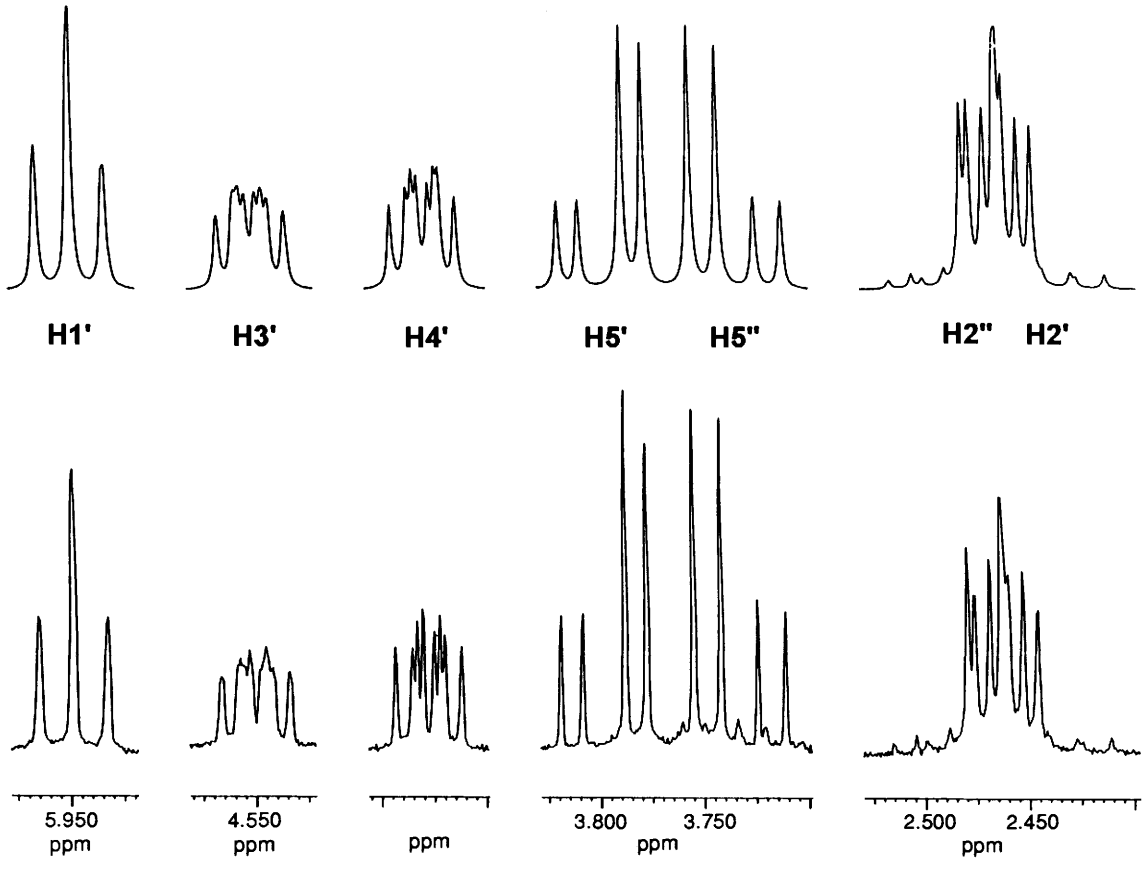

Fig. 1 400.13 MHz ^{1}H NMR spectra of 2-amino-5-[(2-deoxy-β-D-*erythro*-pentofuranosyl)amino]-4*H*-imidazol-4-one **2**, dIz, in D_2O. Bottom: experimental spectrum. Top: simulated spectrum.

Table 3 ^{13}C NMR chemical shifts (ppm) and coupling constants (Hz) of dGuo **1**, dZ **3** and dIz **2**[a]

δ(ppm)	C-6	C-2	C-4	C-8	C-5	C-4′	C-1′	C-3′	C-5′	C-2′
dGuo **1**	156.8	153.6 br[d]	150.7	135.3 ^1J = 212.7[b]	116.7 ^3J = 11.4[c]	87.6 ^1J = 148.7	82.6 ^1J = 169.9	70.8 ^1J = 150.7	61.7 ^1J = 140.5	39.7 ^1J = 132.4
dZ **3**		166.3 br	156.1 br		160.1	86.7 ^1J = 149.2	81.6 ^1J = 163.2	71.0 ^1J = 146.0	62.1 ^1J = 139.4	39.6 ^1J = 132.6
dIz **2**		184.8 br	176.7		166.5 br	87.4 ^1J = 146.0	83.7 ^1J = 162.2	70.9 ^1J = 147.2	62.0 ^1J = 138.5	39.3 ^1J = 131.6

[a] All spectra were obtained in [$^2H_6$]DMSO at 100.57 MHz. [b] ^1J Refers to ^1J(C,H). [c] ^3J-Value is the coupling constant between C-5 and 8-H. [d] br Denoted broadened resonance either with coupling constant less than 2–3 Hz and/or due to the electric quadrupole moment of the ^{14}N nucleus.

anomeric 1-H′ proton. This observation is consistent with the opening of the imidazole ring of the starting dGuo **1**. In addition, a broad signal involving four exchangeable protons (δ = 7.62) may be accounted for by two equivalent amino groups on the sp^3 carbon C-2 of the base moiety of dZ **3**. Further structural information was inferred from two-dimensional ^1H–^{15}N NMR experiments (*vide infra*). In the case of dIz **2**, two other exchangeable protons were observed in the low-field region of the spectrum (δ = 9.06 and 8.94). These protons were attributed to 2-NH and 3-NH, respectively, on the basis of two-dimensional ^1H–^{15}N NMR experiments (*vide infra*). Furthermore, the half-height linewidth of the latter resonance signal at δ = 8.94 was 6.76 Hz whereas that of the 2-NH signal was 32.81 Hz. This could be tentatively explained by a stronger electric quadrupole moment of the ^{14}N imine-type nucleus[22] giving rise to a highly efficient relaxation mechanism. In addition, a slow exchange rate, on the NMR time-scale, of the 2-NH proton cannot be ruled out. The downfield shift of the protons of the base moiety of dIz **2** together with a minor deshielding effect on 1′-H suggested a higher aromaticity of the base moiety of dIz **2** with respect to dZ **3**. This was confirmed by considering the UV absorbance features of compounds **2** and **3**: the spectrum of dIz **2** exhibits a maximum at 254 nm whereas that of dZ **3** shows a decrease in the absorbance within the 200–300 nm range, with a shoulder at 232 nm.

^{13}C NMR spectroscopy. Comparison of the ^{13}C NMR spectra of dGuo **1** and those of dIz **2** and dZ **3** did not show any drastic changes in the chemical shifts of the carbon atoms of the sugar moieties. The assignment of the latter ^{13}C resonance signals was inferred from selective proton-decoupling experiments and further confirmed by ^1H–^{13}C heteronuclear scalar-correlated 2D NMR experiments (see Table 3). The most striking differences occurred within the base moiety of compounds **2** and **3**. Inspection of the low-field region of the spectra of both dIz **2** and dZ **3** reveals the loss of two carbon atoms with respect to the starting dGuo **1**. Moreover, all the remaining carbons are quaternary. They were unambiguously attributed by heteronuclear ^1H–^{13}C multiple-bond-correlation NMR spectroscopy. For dZ **3**, the signal at δ_C 156.1 was assigned as that of C-4 taking into consideration the three- and two-bond correlations with 1′-H and 4-NH respectively (Fig. 2). Another three-bond correlation of the latter 4-NH proton allows the assignment of the signal at δ_C 160.1 as the C-5 carbonyl. Obviously, the last signal which resonates at δ_C 166.3 is that of C-2. Observation of a broadening of this signal, even in the broad-band ^1H-decoupled ^{13}C NMR spectrum of dZ **3**, may be corroborated with the strong electric quadrupole moment of the three ^{14}N nuclei in the α position. A similar observation was made with the broad-band ^1H-decoupled ^{13}C NMR spectrum of dIz **2**. Thus, the signal at δ_C 184.8 was assigned as the imine-type C-2 for which a strong electric quadrupole moment[23] is expected. On the other hand, the very sharp signal resonating at δ_C 176.7 was attributed to the C-4 carbonyl. Assignment of the remaining C-5 carbon atom was obtained from the observation of a three-bond correlation with the 1′-H proton. No correlation was observed with the 5-NH proton, probably because the latter proton is in slight exchange with traces of water. As already described for the ^1H NMR features, the downfield shift of the carbon resonances of dIz **2** with respect to those of dZ **3** is explained by the higher aromaticity of the base moiety of dIz **2**.

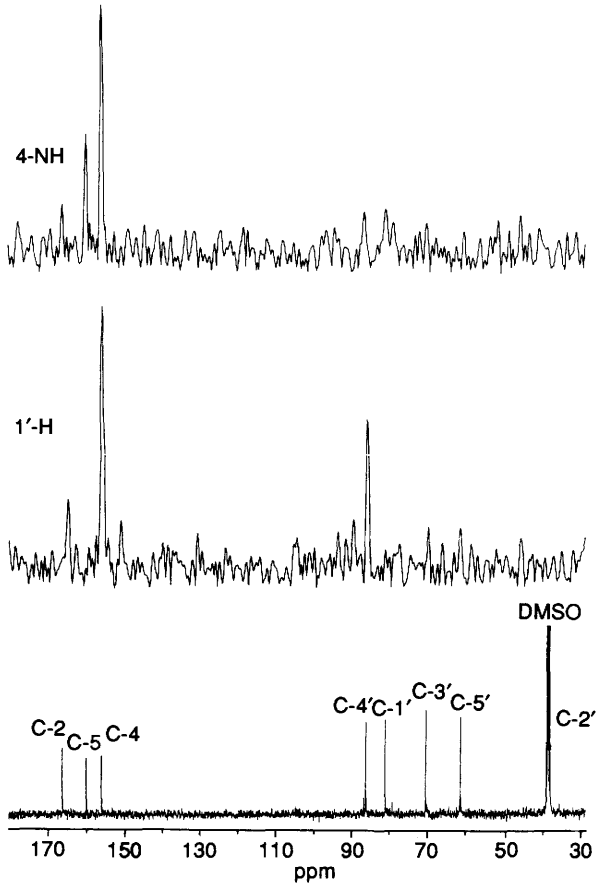

Fig. 2 Long-range ^1H–^{13}C scalar-correlated 2D NMR spectrum (recorded with the HMBC sequence) of dZ **3** in [$^2H_6$]DMSO; only rows showing the protons of interest are plotted. The broad-band ^1H-decoupled ^{13}C NMR spectrum is shown at the bottom.

^{15}N NMR spectroscopy. Relevant information about the structure of the base moiety of compounds **2** and **3** was inferred from ^{15}N NMR data obtained either in the direct detection mode or using two-dimensional ^1H–^{15}N correlation experiments. In the latter case, the proton magnetization is detected.[24] The technique allowed us to overcome the sensitivity problems associated with direct ^{15}N detection (low gyromagnetic ratio and low natural abundance).

The ^{15}N NMR spectrum of dZ **3** obtained in [$^2H_6$]DMSO by direct analysis (Fig. 3) reveals the presence of three distinguishable signals (Table 4). The ^{15}N signal at δ_N −282.7 [^1J(N,H) = −75.1 Hz] was readily assigned as that of the two equivalent NH_2 groups at C-2. The one-bond NH_2-proton scalar correlation with the latter signal confirmed its attribution. For the same reason, the resonance signal at δ_N

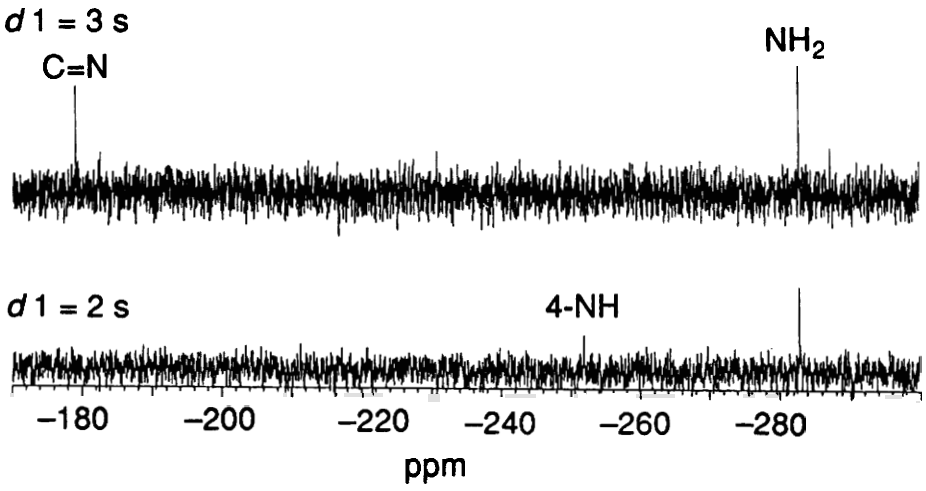

Fig. 3 Direct 50.7 MHz ^{15}N NMR spectra of dZ **3** in [$^2H_6$]DMSO (47 mmol dm^{-3}) recorded with a recycle delay of 2 and 3 s

−251.9 [^1J(N,H) = −133.0 Hz] was assigned to the nitrogen atom of the 4-NH group (Fig. 4). The third signal (δ_N = −179.0) resonating in the low-field region of the spectrum corresponds to a >C=N– imine-type nitrogen atom. In addition, a three-bond scalar correlation with the 4-NH proton allowed the unambiguous attribution of this nitrogen atom to N-3 to be made.

It should be noted that the imidazolone derivative dIz **2** has the ability to exchange very efficiently its labile amino proton atoms, a process which affected the ^{15}N spectroscopic features. Direct ^{15}N NMR experiments confirmed the existence of, at least, two nitrogen atoms. However, the two signals (δ_N −265.4 and −256.3) are very broad (half-height linewidth of ~ 50 Hz) with a poor signal-to-noise ratio of 2.5. The resonance at δ_N −265.4 was readily assigned as N-3 through its one-bond ^1H scalar correlation with the sharpest 3-NH proton at δ_H 8.94 (Fig. 5). The assignment of the –NH–CO– nitrogen atom (δ_N −265.4) is fully consistent with values of ^{15}N chemical shifts of a γ-lactam (δ_N −266.3[25]). This provides further confirmation of a γ-lactam structure for dIz **2**. The three-bond correlation of the 3-NH proton with the ^{15}N resonance at δ_N −179.7 allowed the assignment of the latter signal as N-1, which is very similar to the N-3 of dZ **3**, to be made. Indeed, no confusion is possible with the other imine-type N-2 nitrogen atom which is also three bonds distant and, hence, which should resonate at higher field due to the presence of a proton. A weak scalar correlation was observed between the 3-NH proton and a signal at δ_N −213.8. The latter resonance could be attributed to the N-2 atom. The signal at δ_N −256.3 was assigned as that of N-5 by comparison with the results obtained for the same nitrogen atom (N-4, δ_N = −251.9) in the case of dZ **3**. Indeed, the proton bound to the latter atom being in exchange with residual water, no direct correlation is observable.

^{17}O NMR spectroscopy. The use of ^{17}O-enriched dZ **3** provided further support for the oxazolone structure of this modified nucleoside. The presence of two distinct ^{17}O resonance signals at δ_C = 297.5 (half-height linewidth $w_{\frac{1}{2}}$ = 560 Hz) and δ_O = 283.7 ($w_{\frac{1}{2}}$ = 530 Hz) excluded a ring-open carboxylic acid. In the latter case, only one ^{17}O signal for this functional group should be detected. It should be remembered that the equivalence of the two oxygens of a carboxylic group has been attributed to a fast proton-exchange process.[26] However, an explanation has to be provided for the observation of the two signals obtained for compound **3**. The ^{17}O chemical shifts are very sensitive to the torsion angles and the effect of substituents (*e.g.* –N= and –NH_2 groups), in particular for single-bonded oxygen atoms.[27] Nevertheless, the signal resonating at the lowest field (δ_O 297.5) is likely to be that of C=O while that resonating at the highest field (δ_O 283.7) is attributed to the –O– atom, as expected for a lactone.

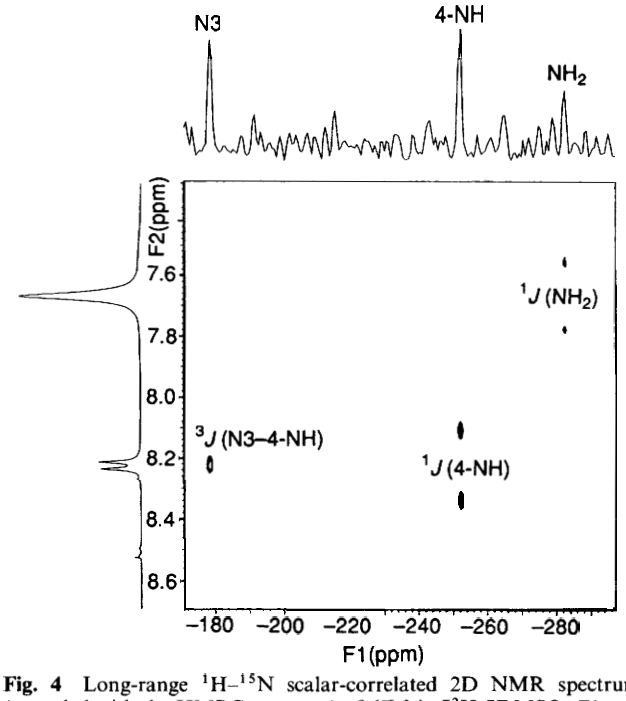

Fig. 4 Long-range ^1H–^{15}N scalar-correlated 2D NMR spectrum (recorded with the HMBC sequence) of dZ **3** in [$^2H_6$]DMSO. *F*1 and *F*2 are the ^{15}N and ^1H dimensions respectively. ^1J(N–H) are residual intense correlations.

Table 4 ^{15}N **NMR chemical shifts**[a] of dGuo **1**, dZ **3** and dIz **2** obtained in [$^2H_6$]DMSO

δ(ppm)	NH-1	NH_2	N-3	N-7	N-9
dGuo **1**	−227.4	−301.5	−208.8	−126.4	−201.1

δ(ppm)	N-3	NH-4	$2NH_2$
dZ **3**	−179.0	−251.9	−282.7

δ(ppm)	N-1	NH-2	NH-3	NH-5
dIz **2**	−179.7	−213.8	−265.4	−256.3

[a] In ppm on the CH_3NO_2 scale

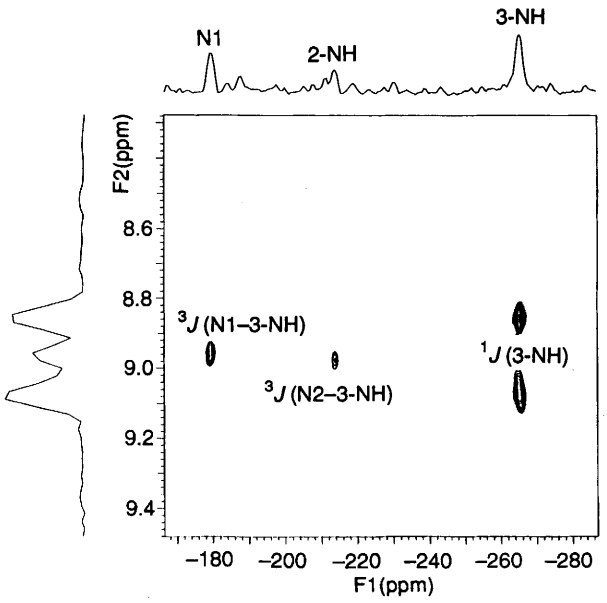

Fig. 5 Long-range ^1H–^{15}N scalar-correlated 2D NMR spectrum (recorded with the HMBC sequence) of dIz **2** in [$^2H_6$]DMSO. *F*1 and *F*2 are the ^{15}N and ^1H dimensions respectively. ^1J(N–H) are residual intense correlations.

Conclusions. In summary, the spectrometric data gathered for the two photooxidized products can be rationalized in terms of the structure proposed for 2,2-diamino-4-[(2-deoxy-β-D-*erythro*-pentofuranosyl)amino]-2,5-dihydrooxazol-5-one **3** and 2-amino-5-[(2-deoxy-β-D-*erythro*-pentofuranosyl)amino]-4*H*-imidazol-4-one **2**, respectively. In addition, the presence of a 2-deoxyribose unit in a β furanose configuration may be inferred from the analysis of the ^1H and ^{13}C NMR spectra of the two compounds. Inspection of the low-field region of the ^{13}C NMR spectra reveals the presence of three quaternary carbon atoms for compounds **2** and **3**. The ^{15}N NMR features of dZ **3** give clear evidence for two equivalent NH_2 groups whereas dIz **2** exhibits a –NH–CO– and a >C=NH group. Both compounds have an imine-type >C=N– nitrogen atom bound through a carbon to an –NH– group in the α position of the anomeric 1′-H proton. The observation of two ^{17}O resonances provided evidence for a ring-closed oxazolone structure for dZ **3** as opposed to a ring-opened carboxylic acid structure. It should also be added that a brown colouration was observed for compound **3** after spraying of the silica gel TLC plates with the hydroxylamine–iron(III) chloride dying reagent. This is specific for the detection of lactones.[28] Additional structural information was inferred from the chemical properties of the two molecules **2** and **3** (*vide infra*).

Chemical properties of dIz 2 and dZ 3

Hydrolysis of dIz 2 to dZ 3. The initially generated oxidized nucleoside, namely the imidazolone derivative dIz **2**, was shown to be unstable in neutral aqueous solution. Hydrolysis of dIz **2**, which is accompanied by the incorporation of one molecule of water, leads to the formation of the oxazolone derivative dZ **3**. This was inferred from an experiment involving the use of labelled $H_2{}^{17}O$. ^{17}O NMR analysis of the ^{17}O-enriched oxazolone **3** revealed the presence of the ^{17}O atom at both >C=O and –O-positions in ~1:1 ratio. The mechanism of generation of dZ **3** involved the transient formation of a weak carboxylic acid as the result of the well known hydrolysis mechanism of a lactam. The negative charge of the latter weak acid is evenly distributed over both oxygen atoms. The two nucleophilic oxygens can attack the electrophilic imino-type carbon atom with similar probability. This intramolecular cyclization leads to the formation of the oxazolone derivative **3** which is ^{17}O-labelled at two positions as depicted in Scheme 2.

Table 5 Half-life $t_{\frac{1}{2}}$ (min)[a] of dIz **2**, dZ **3** and 8-oxodGuo **4** at various conditions of pH and temperature (θ/°C)

Conditions				
pH	θ (°C)	dIz **2**	dZ **3**	8-oxodGuo **4**
7	20	24 h	stable	stable
	37	147	stable	stable
10	65	5.0 (11.2)[b]	21.8	stable
13	20	68.6	20.2 (58.5)[b]	n.d.[c]
	37	26.7	5.1 (23.8)[b]	n.d.
	65	3.1	3.3	38.6

[a] $t_{\frac{1}{2}}$ was calculated from the determination of the slope of the plot $\ln(A_t - A_\infty)$ *versus* time. [b] The value in parentheses represents the second slope of the plot. [c] Not determined.

In fact, a 43/57 relative yield was observed, as inferred from the integration of the two deconvoluted signals (see Fig. 6). Indeed, because of the kinetic isotope effect, intramolecular cyclization by ^{17}O is slightly favoured over cyclization by ^{16}O and explains the slightly greater yield of ^{17}O incorporation at O-1 over >C=O. Kinetic measurements of the hydrolysis of dIz **2** at different temperatures were monitored by UV absorbance of dIz **2** as a function of time (see Fig. 7). The presence of a well defined isosbestic point (λ = 234 nm) is indicative of a single transformation pathway from dIz **2** to dZ **3**, in constant proportions. Such a reaction may be described by pseudo-first-order hydrolysis kinetics. Since dIz **2** exhibits an absorption maximum at 254 nm whereas dZ **3** weakly absorbs at this wavelength, it was possible to follow the decomposition of dIz **2** as a function of time (A_t). Therefore, the slope of the plot of $\ln(A_t - A_\infty)$ *versus* time is accounted for by a pseudo-first-order rate constant k. The rate constant k was determined to be 78.5 μs^{-1} (*i.e.* the half-life time $t_{\frac{1}{2}}$ = 2.5 h) at 37 °C, and 0.029 h^{-1} ($t_{\frac{1}{2}}$ = 24 h) at 20 °C (see Table 5).

Alkali-lability. Both compounds **2** and **3** were very sensitive to alkali treatment. When incubated in alkaline aqueous solution (pH ≥ 10), dIz **2** and dZ **3** decompose quantitatively by releasing the guanidine residue **5**. Measurement of the UV absorbance decay of compounds **2** and **3** allowed the determination of the kinetic parameters of the decomposition to be made. The half-life ($t_{\frac{1}{2}}$) was determined as previously described (*vide infra*) and the resulting data are summarized in Table 5. It should be noted that no isosbestic point was observed under the alkaline conditions used. This is indicative of a complete breakdown of the two molecules **2** and **3**. Nevertheless the coefficient of linear correlation r^2 of each plot was always greater than 0.990 pointing out a pseudo-first-order reaction. In some cases, the hydrolysis seems to proceed *via* a two-step reaction as the result of the observation of two distinct slopes in the curve $\ln(A_t - A_\infty)$ *versus* time. Interestingly, under alkaline conditions (pH ≥ 10), dIz **2** decomposed directly into guanidine **5** without the transient formation of the oxazolone derivative **3**. It should be noted that under drastic conditions (pH 13; 65 °C), the decomposition rate of 8-oxodGuo **4** is more than 10-fold lower. Interestingly, whereas dIz **2** and dZ **3** decompose in buffered pH 10 solution at 65 °C, 8-oxodGuo **4** is particularly stable under these conditions.

The release of guanidine **5** from either compounds **2** or **3** was quantitative upon drastic alkaline treatment (pH 14) for 10 min at 65 °C ($t_{\frac{1}{2}}$ = 3.1 min and 3.3 min, respectively). This property allowed the quantitative determination of the overall formation of the two radical-oxidation products **2**, **3** to be undertaken. For this purpose, an adaptation of a method described for a postcolumn detection of guanidine **5** was used.[29] 1,2-Naphthoquinone-4-sulfonic acid (NQS) reacts quantitatively with guanidine **5** in alkaline solution to yield the highly intense fluorescent derivative **6** (see Scheme 3). The accuracy of the measurement is based on the specificity of the reaction, the retention time of the resulting adduct **6** and also its fluorescent

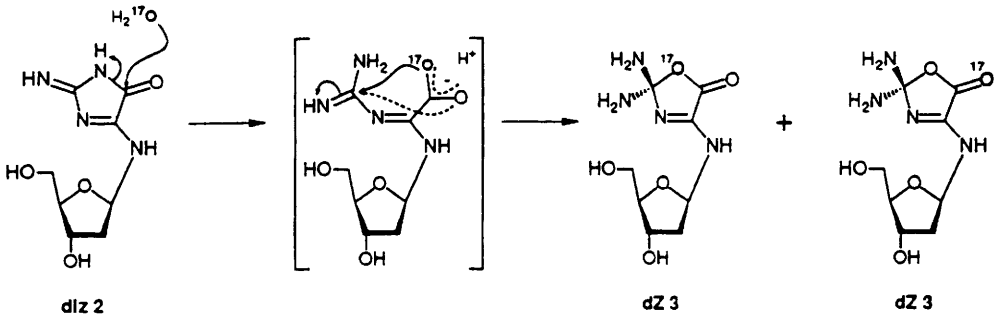

Scheme 2 Mechanism of the hydrolysis of the imidazolone **2** to give the oxazolone **3**

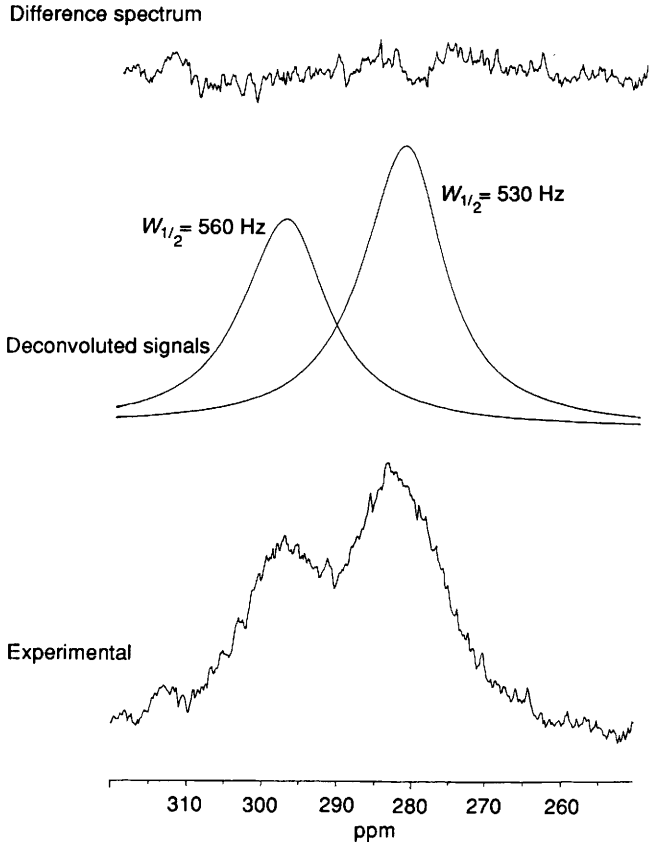

Fig. 6 Low-field region of the 40.7 MHz ^{17}O NMR spectra of ^{17}O-enriched dZ **3** in [$^2H_7$]DMF at 75 °C. Bottom: experimental spectrum. Middle: simulated deconvolution of each of the two resonance signals. Top: difference spectrum.

properties (excitation and emission wavelength detection). The calibration curve obtained with standard samples of commercially available guanidine **5** showed a linear response ($r^2 > 0.997$). The sensitivity of the measurement was determined to be 1 pmol. The calibration curve obtained from a standard aqueous solution of dZ **3** was identical with that previously obtained with guanidine **5**. This relevant information confirms the structure of dIz **2** and dZ **3** and validates the method of detection.

Reactivity towards methoxyamine. The reaction of apurinic DNA with methoxyamine is a well established method to detect apurinic sites.[30-34] Methoxyamine has been shown to react specifically with the aldehyde function of the tautomeric ring-open form of 2-deoxy-D-*erythro*-pentose.[35] It should be added that 3′,5′-di-*O*-acetyl-dIz **2a** is very sensitive to methoxyamine. Interestingly, the methoxyamine treatment of 3′,5′-di-*O*-acetyl-dIz **2a** led to the formation of compounds **7a–d**. However, the HPLC analysis of the crude mixture showed only two peaks with capacity factors, k', of 3.0 and 3.6, respectively. Interestingly, 3′,5′-di-*O*-acetyl-dIz **2a** ($k' = 1.5$) was totally converted into the methoxyamine adducts **7a–d** (*vide infra*) within 5 min. The measurement of the UV absorbance decay indicated a snapshot degradation of the initial product. The positive FAB-mass spectra of the products **7a–d** corresponding to the two HPLC peaks were similar. In particular, they both exhibited a pseudomolecular ion at *m/z* 248.0 (100%, $[M + H]^+$), a glycerol adduct at *m/z* 340.1 (15%, $[M + \text{glycerol} + H]^+$) and a dimeric adduct at *m/z* 495.0 (10%, $[2M + H]^+$). This is indicative of a relative molecular mass of 247 which corresponds to a 3,5-di-*O*-acetyl-2-deoxy-D-*erythro*-pentose–methoxyamine adduct structure. Further support for this assignment was provided by detailed ^1H NMR spectroscopic analyses. The 600.13 MHz ^1H NMR spectrum of the first HPLC fraction obtained in D_2O exhibits three sugar forms, whereas the spectrum of the second HPLC peak shows four sugar forms. The latter ^1H NMR features include the three osidic structures obtained in the first HPLC fraction, in addition to another one. It should be noted that the fourth sugar form appears in the spectrum of the first HPLC fraction when the related content was left in aqueous solution at 20 °C for a few hours. This is indicative of the occurrence of an equilibrium between the four methoxyamine–sugar adducts **7a–d**. Most interestingly, we can observe two different sets of resonance signals for the 1′-H protons. One set corresponding to two forms in equilibrium involves the resonance signals at δ 7.66 and 7.62. It is likely that the two other signals resonating at δ 7.05 and 7.03 are related to a second type of structure. It is interesting to note that these chemical shifts are shifted 1.7 ppm and 1.1 ppm downfield with respect to the corresponding 1′-H resonance signal of 3′,5′-di-*O*-acetyl-dIz **2a**. Such a large downfield shift could be explained by the loss of the aglycone moiety and a nucleophilic addition of the methoxyamine to 3,5-di-*O*-acetyl-2-deoxy-D-*erythro*-pentose. The four methoxyamine–sugar structures observed could be a mixture of the β and α furanose anomers **7a** and **7b** together with the *E* and *Z* isomers **7c** and **7d** of the ring-open iminic tautomer (Scheme 4).

Interestingly, 3′,5′-di-*O*-acetyl-dZ **3a** was less sensitive to methoxyamine treatment than 3′,5′-di-*O*-acetyl-dIz **2a**. It should be noted that the same 3,5-di-*O*-acetyl-2-deoxy-D-*erythro*-pentose–methoxyamine adducts were obtained upon incubation of 3′,5′-di-*O*-acetyl-dZ **3a** with methoxyamine. However, the quantitative conversion of 3′,5′-di-*O*-acetyl-dZ **3a** into 3,5-di-*O*-acetyl-2-deoxy-D-*erythro*-pentose–methoxyamine adducts required a much larger incubation period (*ca.* 10 h).

The hypothetical mechanism for the reaction of methoxyamine with 3′,5′-di-*O*-acetyl-dIz **2a** involves (i) amino nucleophilic attack of the methoxyamine on the base moiety, (ii) the resulting reaction product(s) is (are) much more susceptible to the hydrolysis of the N–glycosidic bond, (iii) a second methoxyamine molecule reacts with the apurinic site, giving rise to the products **7a–d** in equilibrium.

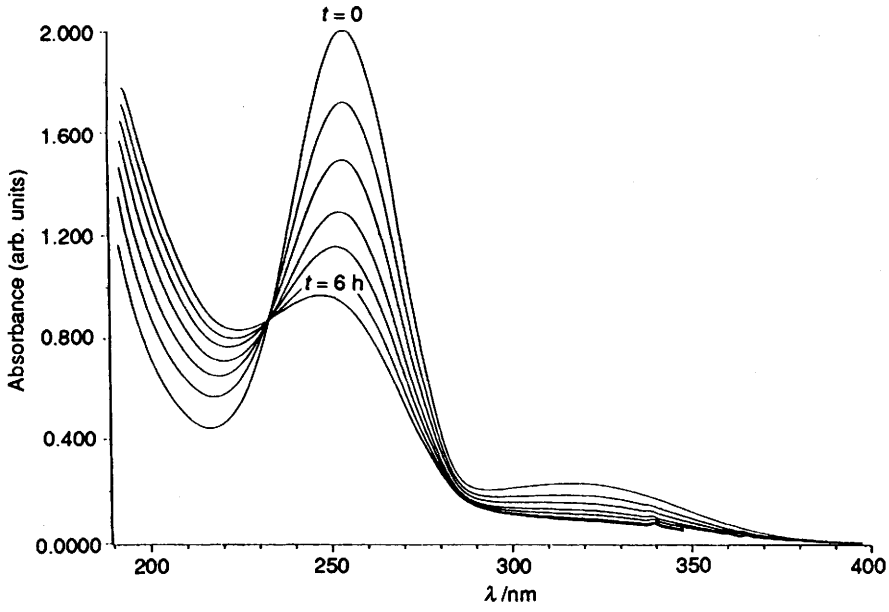

Fig. 7 UV absorbance spectrum, as a function of time, of a neutral aqueous solution of dIz **2** at 37 °C

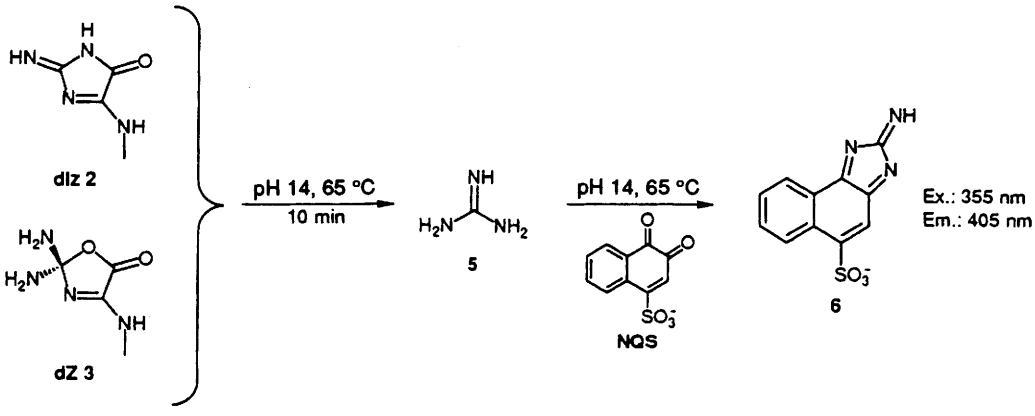

Scheme 3 Chemical detection of dIz **2** and dZ **3**: formation of the fluorescent derivative **6**

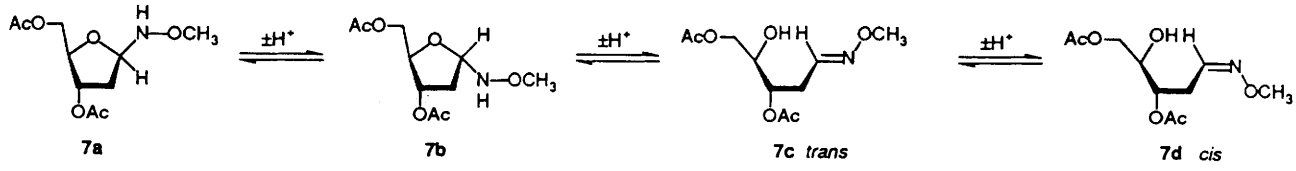

Scheme 4 Equilibrium of the four isomers of the 3,5-di-*O*-acetyl-2-deoxy-D-*erythro*-pentose–methoxyamine adduct

Conclusions

Emphasis was placed in this work on the determination of various spectroscopic features of the main radical-oxidation products of dGuo **1**, an oxazolone derivative **3** and its precursor, an imidazolone derivative **2**. Taken together, these measurements, including FAB-mass determination, UV spectra and mainly multi-nuclei NMR studies, provided further structural evidence for the two oxidized dGuo nucleosides. This supplements the information reported in a previous paper[9] in which the mechanism of formation of compounds **2** and **3** is described in detail. It should be pointed out that the oxidation products of dGuo **1** arise from either one-electron oxidation (Type I photosensitization) or $^{\bullet}OH$ radical oxidation (γ-radiolysis of an aqueous aerated solution). In both cases, dZ **3** and its precursor dIz **2** represent more than 80% of the degradation products of the base moiety of dGuo **1**. Complementary experiments, based on the chemical detection of guanidine, have shown that the oxazolone **3** and imidazolone **2** nucleosides together with 8-oxodGuo **4** are also formed within double-stranded DNA as the result of both $^{\bullet}OH$ and Type I photosensitization reactions. Under these conditions, the relative ratio [oxazolone : 8-oxodGuo] is about [1 : 1] whereas 8-oxodGuo **4** is produced in trace amounts upon γ-irradiation or Type I photosensitization of dGuo **1** in aqueous solution.[36]

In addition, chemical features with emphasis on the stability of the two molecules **2** and **3** were determined. dIz **2** is quantitatively hydrolysed into the stable dZ **3** when left in neutral aqueous solution. Interestingly, both compounds **2** and **3** are highly alkali-labile. They quantitatively decompose into guanidine **5** upon alkali treatment (pH $\geqslant$ 13) as inferred from the measurement of their half-lives at 65 °C, which were estimated to be *ca.* 3 min for both compounds. The alkali-lability shared by both the oxazolone **3** and imidazolone **2** is likely to explain, at least partly, the induction of strand-breaks when oxidized DNA is incubated in alkaline solutions. In this respect, 3-ethoxycarbonylpsoralen-mediated photosensitization of DNA has been shown to induce specific strand-breaks at guanine sites after treatment with hot piperidine.[37] Moreover,

camptothecin + UV-A irradiation induced DNA cleavage exclusively at guanine sites. Interestingly, DNA nicking was markedly enhanced upon treatment with hot piperidine.[38] It may be added that dZ **3** and/or more probably its precursor dIz **2** are the likely unstable and alkali-labile lesions formed in DNA at guanine residues upon photochemical co-sensitized electron transfer by ethidium bromine and methyl viologen.[8] It has to be stated that treatment of photosensitized DNA with hot piperidine is the approach used to detect the overall guanine damage in the DNA-sequencing methodology.[39] We have shown that 8-oxodGuo **4** is 10-fold less sensitive to strong alkali treatment than are dZ **3** and dIz **2** but is stable in buffered pH 10 solution, even at 65 °C. On the other hand, under similar conditions, dZ **3** and dIz **2** decompose within a few minutes. Then, the different alkaline sensitivities of dIz **2**/dZ **3** and 8-oxodGuo **4** should allow the two main classes of guanine-oxidation products to be distinguished: the oxazolone **3**/imidazolone **2** compounds at pH 10 and 8-oxodGuo **4** at pH 13.[40]

The quantitative breakdown of compounds **2** and **3** into guanidine **5** allows the specific detection of the related oxidized DNA damage to occur with a limit of sensitivity which is close to 1 pmol. Analysis of both the main Type I photosensitized dGuo **1** products (dZ **3** and its precursor dIz **2**) and the specific singlet oxygen-mediated oxidation products, the 4*R** and 4*S** diastereoisomers of 2′-deoxy-4-hydroxy-8-oxo-4,8-dihydroguanosine together with the minor 8-oxodGuo **4**,[41] provides an interesting analytical way to determine the ability for a photosensitizer to react *via* a Type I and/or a Type II process.[42,43] In addition, quantitative measurement of compounds **2** and **3** together with that of 8-oxodGuo **4**, upon various oxidation processes, *e.g.* either Type I photosensitized or ·OH-mediated reactions of dGuo **1** in the presence of reducing agents such as ascorbic acid and Fe^{2+}, constitutes another approach to gain insight into mechanistic aspects.[44]

[^{14}C]Methoxyamine is currently used to detect apurinic-apyrimidinic sites in DNA.[30,31] However, we have shown that methoxyamine can react efficiently with dIz **2**, the main degradation product of dGuo **1** generated upon either Type I photosensitization reaction or ·OH radical oxidation under oxic conditions. A possible application of the former reaction may be the quantitative and specific measurement of dIz **2** arising from Type I photosensitization. Indeed, Type I photosensitization is not expected to produce significant numbers of abasic sites in DNA. However, these data clearly showed that the use of methoxyamine assay for the measurement of abasic sites may lead to an overestimation of this class of lesions within oxidized DNA. It has been already shown that 5-formyluracil, a radical oxidation product of thymine,[2] can also efficiently react with another abasic site reagent.[35]

It should be added that attempts are currently underway in our laboratory to establish whether dIz **2** and its decomposition product dZ **3** are recognized and excised by either the formamidopyrimidine-DNA glycosylase (the Fpg protein)[45,46] or other repair enzymes.[47]

Experimental

Chemicals

dGuo **1** was purchased from Pharma-Waldhof (Düsseldorf, Germany) and was used without purification. Benzophenone, NQS and guanidine **5** were obtained from Sigma Chemical Company (St Louis, MO). Methoxyamine hydrochloride was purchased from Aldrich (Steinheim, Germany), NaH_2PO_4 was from Prolabo (France). HPLC-grade methanol and acetonitrile were obtained from Carlo Erba (Farmitalia Carlo Erba, Milan, Italy). Deuterium oxide (D_2O, 99.96% D), heptadeuteriated dimethylformamide ([$^2H_7$]DMF, 99.96% D) and hexadeuteriated dimethyl sulfoxide ([$^2H_6$]DMSO, 99.96% D) used for NMR spectroscopy were purchased from Eurisotop (St Aubin, France). Water was deionized using a Millipore Milli-Q system. $H_2{}^{18}O$ and $H_2{}^{17}O$ were obtained from Eurisotop.

8-OxodGuo **4** was prepared by hydrogenation of 8-benzoyloxy-2′-deoxyguanosine as previously described by Lin *et al.*[48] 3′,5′-Di-*O*-acetyl-dGuo **1a** was synthesized by acetylation of dGuo **1** according to an adaptation of the general procedure described by Johnston.[49]

HPLC analysis

Several pieces of HPLC equipment were used for both analytical and preparative separations. Pre-purification of photosensitized decomposition products of dGuo **1** on a large scale (~200 mg) was achieved using a model PrepLC/System 500 HPLC preparative pumping apparatus equipped with a differential refractometer (Waters Associates, Millipore, Milford, MA) and a Prep/Pack 500 (300 × 50 mm id) octadecylsilyl (ODS) silica gel column (Millipore). The eluent was plain water (pH 6) and the flow rate was set at 100 cm^3 min^{-1}. Further semi-preparative and analytical purifications of the photooxidized nucleosides were accomplished using two model 302 HPLC pumps connected to a model 811 dynamic mixer (Gilson, Middelton, WI), a model LP-21 pulse damper (Scientific System Inc., State College, PA), a Sil-9A automatic injector (Shimadzu Corporation, Kyoto, Japan) and either an L-4000 UV variable-wavelength spectrophotometer (Merck, Darmstadt, Germany) or an F-1050 fluorescence spectrophotometer (Hitachi, Tokyo, Japan). These instruments were connected to an Apple IIe computer which controlled the mobile-phase composition and the flow rate, usually set at 1 and 3 cm^3 min^{-1} for analytical and semi-preparative separations, respectively. HPLC elution profiles were recorded and the peaks of interest were integrated using a Data Master model 621 (Gilson), which analysed the signal coming from the detector. The integrator was interfaced with the computer through the HPLC system manager software model 704 (Gilson, Middelton, WI). The semi-preparative (250 × 10.0 mm id) reversed-phase column (C_{18} Ultremex, mean particle size 5 μm) was purchased from Phenomenex (Torrance, CA). The analytical (250 × 4.6 mm id) octadecylsilyl silica gel column and the semi-preparative (250 × 10.0 mm id) amino-substituted silica gel (mean particle size 5 μm) Hypersil NH_2 column were obtained from Interchim (Montluçon, France).

Spectroscopic measurements

FT-IR spectra were recorded on a Perkin-Elmer Model 1600 spectrophotometer (Norwalk, Connecticut). UV absorption spectra were obtained in aqueous solutions with a Hewlett-Packard 8452A diode array spectrophotometer (Amsterdam, The Netherlands) working at a sweep rate of 105 nm s^{-1}. For the kinetic determination of hydrolysis experiments, the samples were dissolved in the appropriate buffer solutions in the UV-cell fitted with a cap and then placed in a water bath set at the desired temperature. Then, spectra were recorded as a function of time by removing the UV-cell from the water-bath for 2 s. FAB-MS were recorded in the positive mode with a ZAB 2-SEQ spectrometer (Fisons-VG, Manchester, UK) equipped with a liquid secondary-ion mass spectrometry (LSIMS) source. The molecules were dissolved in a glycerol–thioglycerol matrix containing 0.1 mol dm^{-3} NaI and then desorbed upon exposure to a 35 keV caesium ion beam. The ^{1}H NMR spectra were recorded in the Fourier Transform mode using AMX 600, AM 400 and WM 250 Brüker apparatus. Conformational studies were performed in D_2O and spectral assignments of the proton signals were achieved by homonuclear decoupling experiments. 2′-H and 2″-H proton signals were further assigned on the basis of coupling-constant arguments.[50,51] The 5′-H signal was assigned downfield of the 5″-H signal according to Remin and Shugar.[52] To verify the assignments and to obtain accurate chemical shifts and coupling constants, the spectra were computer-simulated using the iterative LAOCOON III and

PANIC Brüker programs. The chemical shifts were determined with respect to either 3-(trimethylsilyl)-[2,2,3,3-$^2H_4$]propionate sodium salt (TSP) in D_2O or tetramethylsilane (TMS) in [$^2H_6$]DMSO as the internal references (0.00 ppm). The proton-coupled and -decoupled ^{13}C NMR spectra and two-dimensional ^1H–^{13}C and ^1H–^{15}N heteronuclear spectra were obtained with a Varian Unity 400 spectrometer. ^{15}N NMR spectra were recorded at 50.7 MHz on a Varian Unity 500 spectrometer using a 10 mm probe. The latter experiments were carried out in [$^2H_6$]DMSO (3.1 cm^3) and required 36 mg of product to be analysed. The recycle delay was set at 3 s and 2 s to overcome the problem of nuclear Overhauser effects. Indeed, with the ^{15}N nucleus owning a negative gyromagnetic ratio (−0.101 relative to protons), it is possible that some signals could be cancelled by the Overhauser effect.[23] For the ^{13}C NMR experiments, the signal of the solvent ([$^2H_6$]DMSO) was used as the secondary reference set at δ_C 39.5. *N*,*N*-Dimethylformamide (DMF) was used as a secondary reference set at δ_N −275.2 with respect to CH_3NO_2, for the ^{15}N NMR experiments.[23] For one-bond and long-range ^1H–^AX (where ^AX = ^{13}C or ^{15}N) scalar-correlated 2D NMR experiments (HMQC and HMBC, respectively), standard Varian software was used. This involved the use of standard pulse sequences provided by the constructor with the parameters indicated below. Theoretically, the optimum delay required to observe long-range correlations in the HMBC experiments is $1/2^nJ(X,H)$, where $^nJ(X,H)$ is the long-range coupling constant. The $^2J(C,H)$ coupling in an aromatic system is usually small (2–3 Hz) whereas $^3J(C,H)$ coupling is within the range 7–15 Hz. Consequently, we used three values (100 ms, 80 ms and 60 ms) for this delay. For ^{15}N, the delay was optimized for $^nJ(N,H)$ = 7 Hz (n = 2 or 3). The delay for polarization transfer in heteronuclear multiple quantum-filtered coherence (HMQC) experiments was set for $^1J(C,H)$ = 167 Hz on the one hand and for $^1J(N,H)$ = 90 Hz on the other. Spectra were recorded at 293–301 K using an indirect 5 mm HX probe. The ^{17}O NMR spectra were recorded on a Brüker AM 300 spectrometer equipped with a 10 mm broadband tuned for ^{17}O at 40.687 MHz. Chemical shifts were measured without proton decoupling and are reported relative to external water used as reference at 75 °C. However, it should be mentioned that the ^{17}O NMR chemical shift of the external reference (H_2O) is 3.3 ppm downfield shifted at 30 °C with respect to the value obtained at 75 °C. 40% ^{17}O-enriched sample of dZ **3** was 0.05 mol dm^{-3} in [$^2H_7$]DMF. The use of high temperatures reduces the linewidth,[53] hence the spectra were recorded at 75 °C. The deconvolution of each resonance signal was obtained using the GLINFIT Brüker program.

Photosensitization procedure

An aqueous solution (750 cm^3) of either 1 mmol dm^{-3} dGuo **1** (200 mg, 0.75 mmol) or 3′,5′-di-*O*-acetyl-dGuo **1a** (263 mg, 0.75 mmol) saturated with benzophenone (0.4 mmol dm^{-3}) was placed in a 1 dm^3 Pyrex tube. Then, the solution was irradiated for 12 h in a Rayonet photoreactor (The Southern New England Ultraviolet Company, Hamden, CT) equipped with 16 'black light' lamps (24 W) emitting ~90% of its light output in the 350 nm range. A continuous air-flow maintained the stirred solution saturated with molecular oxygen (0.25 mmol dm^{-3}). The solution was kept at ~12 °C during irradiation by cooling with a water streamer immersed in the solution. After exposure, the solvent was removed by rotary evaporation (30 °C) and the residue was resuspended in a minimum volume of eluent prior to HPLC analysis. The percentage of degradation of either dGuo **1** or 3′,5′-di-*O*-acetyl-dGuo **1a** was 15%.

2-Amino-5-[(2-deoxy-β-D-*erythro*-pentofuranosyl)amino]-4*H*-imidazol-4-one 2, dIz. Concentration under reduced pressure (30 °C) followed by lyophilization of the main preparative HPLC fraction (capacity factor k' = 3.0) gave dIz **2** (18.2 mg, 11%) as a powder (Found: MH^+, 229.0929. Calc. for $C_8H_{13}N_4O_4$: MH, 229.0937); $\lambda_{max}(H_2O, pH\ 7)$/nm 254; ν_{max}(KBr)/cm^{-1} 3242, 1731, 1640 and 1522; δ_H(400.13 MHz; D_2O) see Table 1; δ_H(250.13 MHz; [$^2H_6$]DMSO) see Table 2; δ_C(100.57 MHz; [$^2H_6$]DMSO) see Table 3; δ_N(50.7 MHz; [$^2H_6$]DMSO) see Table 4; FAB-MS (positive mode, relative intensity) m/z 229 (13%, $[M + H]^+$), 117 (3, $[S]^+$) and 113 (6, $[BH + H]^+$).

2,2-Diamino-4-[(2-deoxy-β-D-*erythro*-pentofuranosyl)-amino]-2,5-dihydrooxazol-5-one 3, dZ. dZ **3** was obtained by leaving the previously isolated dIz **2** in aqueous solution (pH 7) at 37 °C. After complete transformation of compound **2** (24 h), lyophilization of the solution yielded dZ **3** (21.5 mg) as a powder (Found: MH^+, 247.1152. Calc. for $C_8H_{15}N_4O_5$: MH, 247.1042); $\lambda_{max}(H_2O, pH\ 7)$/nm 232 (sh); ν_{max}(KBr)/cm^{-1} 3356, 2945, 1781, 1737, 1659 and 1490; δ_H(400.13 MHz; D_2O) see Table 1; δ_H(250.13 MHz; [$^2H_6$]DMSO) see Table 2; δ_C(100.57 MHz; [$^2H_6$]DMSO) see Table 3; δ_N(50.7 MHz; [$^2H_6$]DMSO) see Table 4; δ_O(40.7 MHz; [$^2H_7$]DMF) 283.7 ($w_{\frac{1}{2}}$ 530 Hz, –O–) and 297.5 ($w_{\frac{1}{2}}$ 560 Hz, =O); FAB-MS (positive mode, relative intensity) m/z 247 (41%, $[M + H]^+$), 131 (7, $[BH + H]^+$) and 117 (4, $[S]^+$).

2-Amino-5-[(3,5-di-*O*-acetyl-2-deoxy-β-D-*erythro*-pento-furanosyl)amino]-4*H*-imidazol-4-one 2a. The separation of the two main 3′,5′-di-*O*-acetyl-dGuo photoproducts **2a** and **3a** was achieved by HPLC on an ODS column (250 × 6.2 mm id) under isocratic conditions using a mixture of water (pH 6) and methanol (75/25, v/v) as the eluent at a flow rate of 2 cm^3 min^{-1}. Under these conditions, the unmodified nucleoside **1a** has k' = 3.5. Lyophilization of the combined fraction (k' = 1.6) provided 3′,5′-di-*O*-acetyl-dIz **2a** (30.1 mg, 13%) as a powder (Found: MH^+, 313.1138. Calc. for $C_{12}H_{17}N_4O_6$: MH, 313.1148); $\lambda_{max}(H_2O, pH\ 7)$/nm 254; ν_{max}(KBr)/cm^{-1} 3287, 1735, 1638 and 1520; FAB-MS (positive mode, relative intensity) m/z 313 (71%, $[M + H]^+$), 201 (29, [3,5-di-*O*-acetyl-2-deoxy-D-*erythro*-pentose]$^+$) and 113 (55, $[BH + H]^+$); the ^1H and ^{13}C NMR data were identical with those previously reported by Cadet *et al.*[9]

2,2-Diamino-4-[(3,5-di-*O*-acetyl-2-deoxy-β-D-*erythro*-pento-furanosyl)amino]-2,5-dihydrooxazol-5-one 3a. The previously obtained fraction containing 3′,5′-di-*O*-acetyl-dIz **2a** was left in neutral aqueous solution at 37 °C for 24 h. Then, the solution was concentrated and lyophilized, to yield 3′,5′-di-*O*-acetyl-dZ **3a** (31.8 mg). Under the same HPLC conditions, compound **3a** has k' = 0.8 (Found: MH^+, 331.1258. Calc. for $C_{12}H_{19}N_4O_7$: MH, 331.1254); $\lambda_{max}(H_2O, pH\ 7)$/nm 232 (shoulder); ν_{max}(KBr)/cm^{-1} 3394, 1737, 1662 and 1490; FAB-MS (positive mode, relative intensity) m/z 331 (81%, $[M + H]^+$), 287 (18, $[M + H - CO_2]^+$), 201 (26, [3,5-di-*O*-acetyl-2-deoxy-D-*erythro*-pentose]$^+$) and 131 (22, $[BH + H]^+$); the ^1H and ^{13}C NMR data were identical with those previously reported by Cadet *et al.*[9]

Chemical detection of guanidine 5

The method is an adaptation of the measurement of guanidine derivatives as initially described for a postcolumn derivatization assay.[29] Typically, 100 mm^3 of photosensitized 1 mmol dm^{-3} dGuo **1** was mixed with 1 mol dm^{-3} sodium hydroxide (50 mm^3). After homogenization, the solution was placed in a water-bath at 65 °C for 10 min. Then, NQS (0.8 mg cm^{-3}; 10 mm^3) was added and the resulting solution was placed at 65 °C for 2 min. The sample was neutralized by addition of 50 μl of mol dm^{-3} hydrochloric acid (50 mm^3) prior to RP-HPLC analysis. The aromatic fluorescent derivative **6** (k' = 5.0) was detected using a fluorescence detector (excitation and emission wavelengths set at 355 and 405 nm, respectively). The eluent was a mixture of 25 mmol dm^{-3} ammonium formate in water and methanol (90/10, v/v). An external calibration was performed using a standard solution of commercially available guanidine **5**. The sensitivity of the method was established to be 1 pmol.

Methoxyamine treatment of 3′,5′-di-*O*-acetyl-dIz 2a and 3′,5′-di-*O*-acetyl-dZ 3a. Acetylated nucleoside **2a** or **3a** (6 mg, 0.02 mmol) was added to 0.25 mol dm^{-3} methoxyamine-buffered solution (pH 7) (1.5 cm^3). Then, the mixture was incubated at

37 °C for 30 min. The reaction was monitored by either direct injection onto the semi-preparative HPLC column for the 3',5'-di-*O*-acetyl-dZ **3a** or UV absorption spectra for 3',5'-di-*O*-acetyl-dIz **2a**. The first fraction containing 1.8 mg (yield 37%) of the three methoxyamine–sugar adducts exhibits a capacity factor of 3.0. Evaporation of the second HPLC eluted peak ($k' = 3.6$) gives the four methoxyamine–sugar adducts **7a–d** (3.1 mg, 62%).

Acknowledgements

We gratefully thank Colette Lebrun for her contribution to mass spectrometry measurements and Michel Bardet for helpful discussions and assistance concerning the ^{17}O NMR experiments. We are also indebted to Marie-Françoise Foray for the 600 MHz ^{1}H NMR analyses and we acknowledge the support of the European Commission CHCM program (contract No. CHRX CT 93 0275).

References

1 L. J. Marnett and P. C. Burcham, *Chem. Res. Toxicol.*, 1993, **6**, 771.
2 J. Cadet, in *DNA Adducts: Identification and Biological Significance*, eds. K. Hemminki, A. Dipple, D. G. E. Shuker, F. F. Kadlubar, D. Segerbäck and H. Bartsch, IARC Scientific Publications, Lyon, 1994, vol. 125, pp. 245–276.
3 B. Meunier, G. Pratviel and J. Bernadou, *Bull. Soc. Chim. Fr.*, 1994, **131**, 933.
4 S. Steenken, *Chem. Rev.*, 1989, **89**, 503.
5 C. S. Foote, *Photochem. Photobiol.*, 1991, **54**, 659.
6 J. Piette, *J. Photochem. Photobiol. B: Biol.*, 1991, **11**, 241.
7 L. P. Candeias and S. Steenken, *J. Am. Chem. Soc.*, 1992, **114**, 699.
8 D. A. Dunn, V. H. Lin and I. E. Kochevar, *Biochemistry*, 1992, **31**, 11 620.
9 J. Cadet, M. Berger, G. W. Buchko, P. C. Joshi, S. Raoul and J.-L. Ravanat, *J. Am. Chem. Soc.*, 1994, **116**, 7403.
10 J. Cadet, M. Berger, B. Morin, J.-L. Ravanat, S. Raoul, G. W. Buchko and M. Weinfeld, *Spectrum*, 1994, **7**, 21.
11 M. C. R. Symons, *J. Chem. Soc., Faraday Trans. 1*, 1987, **83**, 1.
12 L. P. Candeias and S. Steenken, *J. Am. Chem. Soc.*, 1993, **115**, 2437.
13 T. Melvin, S. Botchway, A. W. Parker and P. O'Neill, *J. Chem. Soc., Chem. Commun.*, 1995, 653.
14 L. P. Candeias and S. Steenken, *J. Am. Chem. Soc.*, 1989, **111**, 1094.
15 H. Kasai and S. Nishimura, *Nucleic Acids Res.*, 1984, **12**, 2137.
16 B. P. Cho, F. F. Kadlubar, S. J. Culp and F. E. Evans, *Chem. Res. Toxicol.*, 1990, **3**, 445.
17 R. A. Floyd, M. S. West, K. L. Eneff and J. E. Schneider, *Arch. Biochem. Biophys.*, 1989, **273**, 106.
18 J.-L. Ravanat, T. Douki, M.-F. Incardona and J. Cadet, *J. Liq. Chromatogr.*, 1993, **16**, 3185.
19 C. Altona and M. Sundaralingam, *J. Am. Chem. Soc.*, 1972, **94**, 8205.
20 C. Altona and M. Sundaralingam, *J. Am. Chem. Soc.*, 1973, **95**, 2333.
21 C.-H. Lee and R. H. Sarma, *J. Am. Chem. Soc.*, 1976, **98**, 3541.
22 R. J. Abraham, J. Fisher and P. Loftus, *Introduction to NMR Spectroscopy*, Wiley, Chichester, 1988.
23 G. J. Martin, M. L. Martin and J.-P. Gouesnard, *^{15}N-NMR Spectroscopy*, Springer-Verlag, Berlin, Heidelberg and New York, 1981.
24 A. Bax, R. H. Giffey and B. L. Hawkins, *J. Am. Chem. Soc.*, 1983, **105**, 7188.
25 K. L. Williamson and J. D. Roberts, *J. Am. Chem. Soc.*, 1976, **98**, 5082.
26 C. Delseth, T. T.-T. Nguyen and J.-P. Kintzinger, *Helv. Chim. Acta*, 1980, **63**, 498.
27 D. W. Boykin, *^{17}O NMR Spectroscopy in Organic Chemistry*, CRC Press, Boca Raton, FL, 1991.
28 V. P. Whittaker and S. Wijesundera, *Biochem. J.*, 1952, **51**, 348.
29 Y. Kobayashi, H. Kubo and T. Kinoshita, *Anal. Biochem.*, 1987, **160**, 392.
30 M. M. Coombs and D. C. Livingston, *Biochim. Biophys. Acta*, 1969, **174**, 161.
31 M. Talpaert-Borlé and M. Liuzzi, *Biochim. Biophys. Acta*, 1983, **740**, 410.
32 M. Liuzzi and M. Talpaert-Borlé, in *DNA Repair, a Laboratory Manual of Research Procedures*, ed. E. C. Friedberg and P. C. Hanawalt, Marcel Dekker, New York and Basel, 1988, vol. 3, p. 443.
33 M. Weinfeld, M. Liuzzi and M. C. Paterson, *Biochemistry*, 1990, **29**, 1737.
34 P. Fortini, A. Calcagnile, H. Vrieling, A. van Zeeland, M. Bignami and E. Dogliotti, *Cancer Res.*, 1993, **55**, 1149.
35 H. Ide, K. Akamatsu, Y. Kimura, K. Michiue, K. Makino, A. Asaeda, Y. Takamori and K. Kubo, *Biochemistry*, 1993, **32**, 8276.
36 S. Raoul, M. Berger, G. W. Buchko, J.-L. Ravanat and J. Cadet, *Proceedings of the 18th L. H. Gray Conference*, University of Bath, UK, 10–14 April; *Int. J. Radiat. Biol.*, 1994, **66**.
37 E. Sage, T. Le Doan, V. Boyer, D. E. Helland, L. Kittler, C. Hélène and E. Moustacchi, *J. Mol. Biol.*, 1989, **209**, 297.
38 F. Leteurtre, M. Fesen, G. Kohlhagen, K. W. Kohn and Y. Pommier, *Biochemistry*, 1993, **32**, 8955.
39 A. M. Maxam and W. Gilbert, *Methods Enzymol.*, 1980, **65**, 499.
40 M.-H. Chung, H. Kiyosawa, E. Ohtsuka, S. Nishimura and H. Kasai, *Biochem. Biophys. Res. Commun.*, 1992, **188**, 1.
41 J.-L. Ravanat and J. Cadet, *Chem. Res. Toxicol.*, 1995, **8**, 379.
42 J.-L. Ravanat, M. Berger, F. Benard, R. Langlois, R. Ouellet, J. E. van Lier and J. Cadet, *Photochem. Photobiol.*, 1992, **55**, 809.
43 D. Averbeck, K. Polasa, J.-P. Buisson, R. Bensasson, M. Rougée, J. Cadet, J.-L. Ravanat, F. Perin, P. Vigny and P. Demerseman, *Mutat. Res.*, 1993, **287**, 165.
44 L. P. Candeias and S. Steenken, in *The Early Effects of Radiation on DNA*, ed. E. M. Fielden and P. O'Neill, NATO ARW Series, Springer, Berlin, 1991, vol. 54, p. 265.
45 J. Tchou, V. Bodepudi, S. Shibutani, I. Antoshechkin, J. Miller, A. P. Grollman and F. Johnson, *J. Biol. Chem.*, 1994, **269**, 15 318.
46 S. Boiteux, E. Gajewski, J. Laval and M. Dizdaroglu, *Biochemistry*, 1992, **31**, 106.
47 Z. Hatahet, Y. W. Kow, A. A. Purmal, R. P. Cunningham and S. S. Wallace, *J. Biol. Chem.*, 1994, **269**, 18 814.
48 T.-S. Lin, J.-C. Cheng, K. Ishiguro and A. C. Sartorelli, *J. Med. Chem.*, 1985, **28**, 1194.
49 G. A. R. Johnston, *Tetrahedron*, 1968, **24**, 6987.
50 D. B. Davies and S. S. Danyluk, *Biochemistry*, 1974, **13**, 4417.
51 D. J. Wood, F. E. Hruska and K. K. Ogilvie, *Can. J. Chem.*, 1974, **53**, 3353.
52 M. Remin and D. Shugar, *Biochem. Biophys. Res. Commun.*, 1972, **48**, 636.
53 H. Kählig and W. Robien, *Magn. Reson. Chem.*, 1994, **32**, 608.

Paper 5/04627K
Received 14*th July* 1995
Accepted 21*st August* 1995